Supplementary information for a scale-invariant large-area single-mode topological photonic cavity

Zhongfu Li[1,2†], Shiqi Li[3†], Bei Yan[4†], Hsun-Chi Chan[2†], Jing Li[1], Jun Guan[1], Wengang Bi[1], Yuanjiang Xiang[6], Zhen Gao[4,5*], Shuang Zhang[2*], Peng Zhan[3*], Zhenlin Wang[3], Biye Xie[1*]

[1]School of Science and Engineering, The Chinese University of Hong Kong, Shenzhen, Guangdong, 100190, China.
[2]The New Cornerstone Science Foundation, Department of Physics, The University of Hong Kong, Pokfulam Road, Hong Kong, 999077, China.
[3]Collaborative Innovation Center of Advanced Microstructures and School of Physics, Nanjing University, Nanjing, 210093, China.
[4]Department of Electronic and Electrical Engineering, Southern University of Science and Technology, Shenzhen, Guangdong, China.
[5]State Key Laboratory of Optical Fiber and Cable Manufacture Technology, Southern University of Science and Technology, Shenzhen, Guangdong, China.
[6]School of Physics and Electronics, Hunan University, Changsha, 410082, China.

*Corresponding author(s). E-mail(s): gaoz@sustech.edu.cn; shuzhang@hku.hk; zhanpeng@nju.edu.cn; xiebiye@cuhk.edu.cn;
†These authors contributed equally to this work.

Supplementary Note 1. Tight-binding model and Hamiltonian

In this section, we will give a brief introduction of how to build the tight-binding (TB) model used in the main text. The schematic diagram of one simply TB model consisting of SOTI and DM is shown in Fig. S1(a). First, we need to assign numbers to all the sites (assuming there are N sites). After numbering all the sites, we can

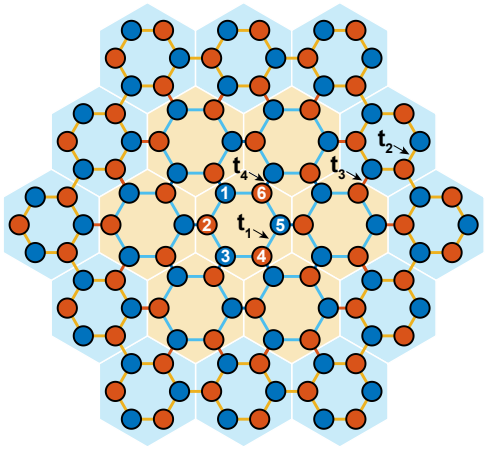

Fig. S1 Schematic diagram of TB model. Different backgrounds represent lattices with different topological phases, where yellow corresponds to topologically non-trivial lattices, and blue represents gapless lattices. Solid lines represent couplings between sites, with different colors indicating varying coupling strengths labeled as t_1 to t_4.

obtain the Hamiltonian (N-by-N) according to the hopping between different sites:

$$H(i,j) = t_l, l = 1, 2, 3, 4, \tag{1}$$

where the value of t_l depends on the hopping between site i and j.

In our TB model, there only exist two types of topological phases with four different strengths of couplings, as illustrated in Fig. S1 with distinct colors. After obtaining the Hamiltonian, we can calculate the eigenvalues and corresponding eigenvectors easily. In the main text, we have shown the results of ψ^2 distribution. Here, we show the results of ψ distribution in Fig. S2. Similar to the results in the main text, as the number of layers of DM increases, the mode area of SSLTC gradually enlarges.

Next, we will explore the properties of cavity consisting of DM as shown in the Fig. 1(b) of main text. First, we can write down the Hamiltonian of the structure based on the steps described above. The hexagonal structure used here has a side length of 5 unit cells, and all coupling strengths are equal to 2. Here, to eliminate the influence of finite size, we have applied special boundary conditions, which has shown in Fig. S3**a**. The main idea is to eliminate the influence of finite size by removing the boundaries. So, we introduced couplings between every pair of boundaries (marked with the same color), and their corresponding eigenvalues are plotted in Fig. S2b. Because the band structure of unit cell used here has a fourfold degenerate point at the Γ point, there are four degenerate eigenvalues labeled as c-f. The energy of these four eigenvalues equal to zero, which protected by chiral symmetry. Corresponding eigenvectors distribution are shown in Fig. S3c-f. All these four states all exhibit the characteristic of a uniform field distribution.

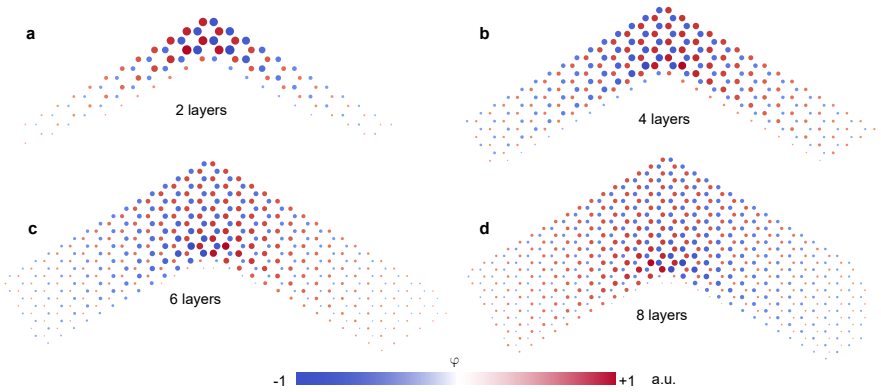

Fig. S2 The eigenvector (ϕ) distribution of the TB model. a, 2 layers DM and 20 layers SOTI. b, 4 layers DM and 20 layers SOTI. c, 6 layers DM and 20 layers SOTI. d, 8 layers DM and 20 layers SOTI.

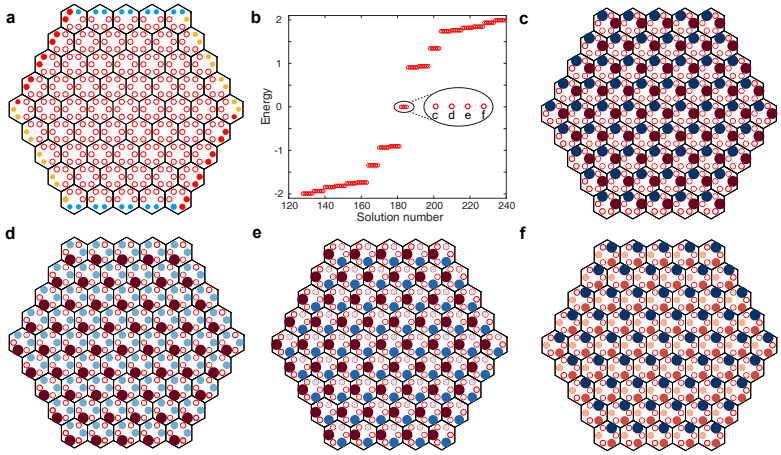

Fig. S3 a, Schematic diagram of TB model consisting of DM, there exist long range couplings between the sites marked by the colored circles. These additional couplings can eliminate all the open boundaries. b, Eigenvalues of structure shown in a, , where exist four degeneracy modes (labeled by c-f). c-f, Corresponding eigenvector distribution of zero-energy states marked in b.

Supplementary Note 2. Full-wave simulation results

In this section, we will present the results of full-wave simulations. The eigenfields of SSLTC with varying numbers of DM layers calculated by using full-wave simulation are depicted in Fig. S4. In all full-wave simulations, PEC boundaries are used to enclose the entire structure. The parameters used in the simulations are consistent with those described in the main text. To align with the experimental setup, we simulated only one corner in the full-wave simulations. In addition, to demonstrate that the appearance of SSLTC does not depend on the parity of the DM layers, we simultaneously provide the results for odd and even layers of DM, as shown in Fig.

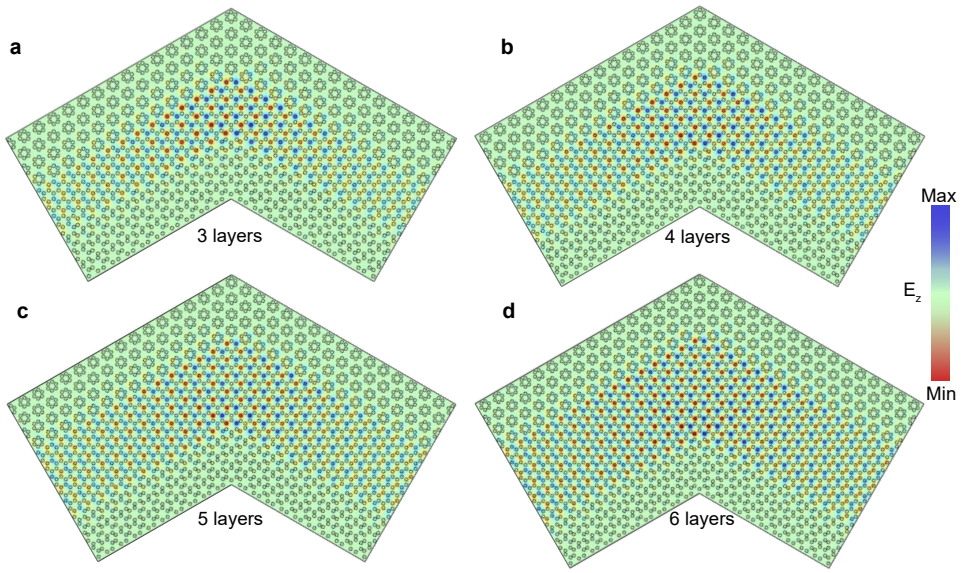

Fig. S4 The eigenfield (E_z) distribution with varying number of DM layers. As the number of layers increases, the SSLTC area gradually expands. a, 3 layers DM, 4 layers OI and 4 layers SOTI. b, 4 layers DM, 4 layers OI and 4 layers SOTI. c, 4 layers DM, 4 layers OI and 4 layers SOTI. d, 4 layers DM, 4 layers OI and 4 layers SOTI.

S4.As evident from the results, as the number of DM layers gradually increases, the mode area also increases, while ensuring consistent chiral eigenvalues.

For the scale-invariant cavity, we also give the corresponding full-wave simulation in Fig. S5. First, the eigenfrequency of cavity is shown in Fig. S5 a. Despite the entire structure being composed of gapless lattices linear bands break up into discrete modes under the influence of finite size effect. And two degeneracy fundamental modes are marked by text b and c, where the eigenfields are shown in Fig. S5b and c.

Finally, we show some other eigenmodes of DM cavity with disorder near the degeneracy frequency in Fig. S6. We observe that the original scale-invariant modes vanish, and the new modes no longer exhibit a uniform field distribution due to the influence of disorder.

Supplementary Note 3. Topological invariants

Higher-order topological invariants provide essential insights into the unique properties of our system. In the realm of topological crystalline insulators (TCIs) characterized by C_n symmetry, higher-order topology is often discerned through the presence of fractional charges [1, 2]. For all three different lattices (expended, shrunken and gapless), we can use a 2D TB model to study the fractional charges. The presence of this rotational symmetry imposes significant constraints on the band structures. Consequently, we can select the eigenstates of the Hamiltonian at high symmetry

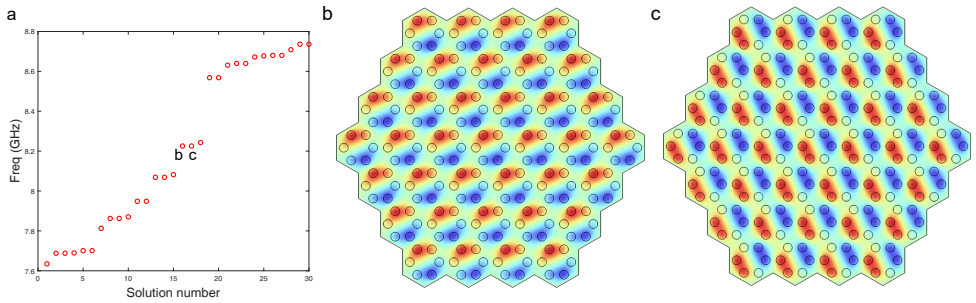

Fig. S5 The eigenfrequency and eigenfields of scale-invariant cavity. There are two degeneracy eigenmodes which are marked by b and c. And the corresponding eigenfields are plotted in b and c.

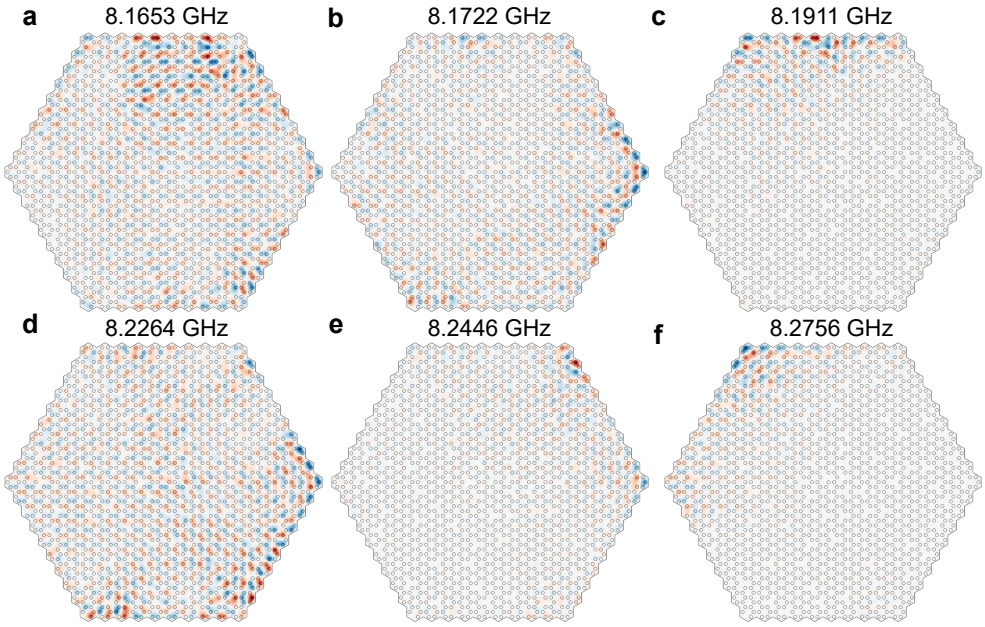

Fig. S6 Six eigenmodes of DM cavity with disorder near the degeneracy frequency. There is no longer a scale-invariant mode under the effect of disorder.

points within the first Brillouin zone (FBZ) same as eigenstates of the six-fold rotation operator, which reads:

$$\Pi_j = e^{2\pi j(p-1)/6}, j = 1, 2, 3, 4, 5, 6, \tag{2}$$

where Π represents high symmetry points in FBZ (K,M and Γ). Form the rotation eigenvalues we can define the bulk polarization and secondary topological indice as:

$$\begin{aligned} P_x &= P_y = [K_1] + 2\,[K_2] = 0 \mod 1 \\ Q^c &= \frac{1}{4}\,[M_1] + \frac{1}{6}\,[K_1] \mod 1 \end{aligned} \tag{3}$$

where $[\Pi_j] = \#\Pi_j - \#\Gamma_j$ and $\#\Pi$ is the number of bands below the bandgap. Next, our attention focus the physics of corners. It is well-established that the combination of two C_n symmetric TCIs results in another TCI. In this case, the rotational representation of the combined system is simply the sum of the rotational representations of the two original TCIs. This free Abelian additive structure in TCI classification offers us the opportunity to select a set of fundamental systems, known as primitive generators, which can be used to generate all TCIs up to a stable equivalence. In the context of our photonic crystals, these primitive generators are represented as $g_{3c}^{(6)}$.

Based on above discussion, we have $[M_1] = 2$ and $[K_1] = 0$, which gives:

$$p_l = 0, Q^c = \frac{1}{2}, \tag{4}$$

Form the Eq. 4, we can find that the dipole moments are vanishing in C_{6v}-symmetric lattice and the topological index is $\frac{1}{2}$, which indicating that there exist second-order topological phase in our system.

References

[1] Benalcazar, W.A., Li, T., Hughes, T.L.: Quantization of fractional corner charge in C n -symmetric higher-order topological crystalline insulators. Phys. Rev. B **99**(24), 245151 (2019) https://doi.org/10.1103/PhysRevB.99.245151

[2] Noh, J., Benalcazar, W.A., Huang, S., Collins, M.J., Chen, K.P., Hughes, T.L., Rechtsman, M.C.: Topological protection of photonic mid-gap defect modes. Nat. Photonics **12**(7), 408–415 (2018) https://doi.org/10.1038/s41566-018-0179-3